STRUCTURAL CHARACTERIZATION OF THE CERBERUS FOSSAE AT THE ATHABASCA VALLES SOURCE REGION, MARS. K. D. Runyon[1], A. K. Davatzes[1], and N. C. Davatzes[1],[1]Temple University, Department of Earth and Environmental Science, 1901 N. 13th St., Philadelphia, PA 19122, kirby.runyon@gmail.com.

Introduction: The Cerberus Fossae have been interpreted as normal fault-bounded graben formed above subcropping dikes [1,2] or alternatively as tension cracks [3]. Pit craters and troughs that extend beyond the tips of the fossae are consistent with overburden collapse due to dilatation above dikes or normal faults growing from depth [4]. Athabasca Valles, one of the large outflow channels, originates at the Cerberus Fossae (Fig. 1) [5], and notably is associated with relays between fossae segments [6].

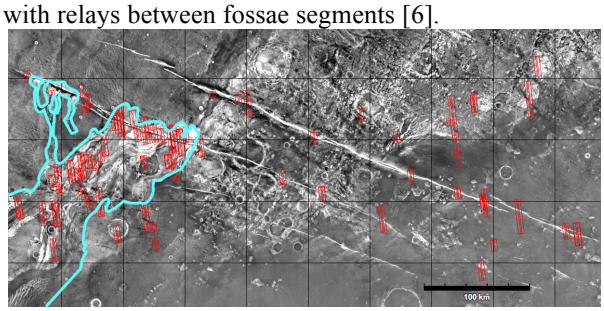

Fig. 1: Cerberus Fossae (diagonal across image) and Athabasca Valles (blue outline) are shown on this nighttime THEMIS mosaic with HiRISE images outlined in red. Grid lines are 1° apart and the scale bar is 100 km. North is up.

In terrestrial normal faults, increased displacement gradients at fault tips and relays between fault segments concentrate crustal stresses [4,7,8] and can cause increased fracture density and fracture-hosted permeability [4,8,9,10]. Such mechanical interaction among normal faults is evidenced by displacement profiles along fault segment strike in which [7,11,12,]: (1) peak displacement is skewed away from the center of the segment toward the neighboring segment or towards the center of the array of segments; (2) where segments overlap, displacement gradient and displacement is lower, but the sum of the displacements of the overlapping segments approximates the displacement of a single larger segment; (3) where segments underlap displacement gradient is increased toward the neighboring segment as compared to a single fault segment. Thus, if the fossae originate as faults, fossae tips and relays should coincide with increased fracture density and the displacement, represented as the difference in height between fossae floor and rim, should show characteristic displacement profiles. This independent evidence of a faulting origin provides a mechanism for developing vertical, high permeability conduits similar to terrestrial faults [8,9,13]. Increased fracture density in the relay associated with mapped outflow at Athabasca Valles similarly provides evidence that fault-controlled permeability played a role in its development.

Displacement profiles: The individual segments of Cerberus Fossae were mapped using high-resolution images from the CTX camera overlain on the THEMIS Day IR global mosaic (Fig. 2a). Three distinct major segments are distinguished, shown in red, green, and black. These major segments appear to be composed of several smaller sub-segments, now linked together, that are revealed by ridges extending into the fossae.

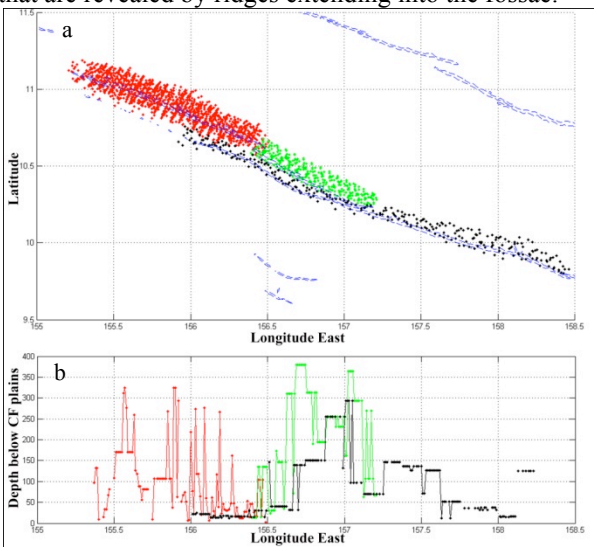

Fig. 2: (a) Map of fossae segments with MOLA data in red, green, and black dots where color corresponds to fossae segments a, b, and c, respectively. (b) Fossae vertical displacement profiles.

The corresponding displacement profiles of these segments were derived from: (1) comparison of elevation of the graben floor and rim from data taken by the Mars Orbiter Laser Altimeter (MOLA) along three sections of the southern Cerberus Fossae (SCF) associated with Athabasca Valles (Fig. 2a) since graben depth should depend on normal fault throw; (2) shadow measurements of the graben floor depth using High Resolution Imaging Science Experiment (HiRISE) images where available. The shadow measurements are consistent with the maximum depth measurements from MOLA.

The elevation difference was plotted against longitude to test whether the fossae behave like terrestrial normal faults. Mapping revealed significant alluvial fan development within the fossae, indicating that current elevation differences generally underestimate throw due to aggradation. To account for this underestimate, the measurements were binned in 0.01 degree longitudinal increments (~600 m) corresponding to the

approximate width of three alluvial fans along the floor of the fossae. The maximum elevation difference within each bin should most closely correspond to fault throw (Fig. 2b).

The segments of the SCF show displacement profiles consistent with the profiles of terrestrial normal faults. In particular, the transition from the western segment (red) to the two eastern segments (green and black) shows that the throw maxima are skewed toward each other; also, the eastern two segments show suppressed displacement and displacement gradient in the overlap. More local peak displacements correspond to the smaller, linked segments recognized during mapping. Adjacent to the relay, displacement gradient is enhanced, especially in comparison to the easternmost segment (black). These characteristics are consistent with a faulting origin of the fossae and further suggest mechanical interaction between the segments.

Fracture Intensity: Fracture intensity along the fossae was measured using high-resolution HiRISE images (Fig. 3). Fractures are characterized by high length-to-width ratio, a different albedo from the surroundings, shading consistent with negative topographic relief, a lack of a raised rim, and non-association with polygonized terrain. These criteria are consistent with open fractures and preclude aeolian and lava features, as well as gravity-driven collapse features, which do not control fluid flow. Fractures were mapped within an area extending one half-fossae width to either side of the fossae (Fig. 3).

Fracture intensity was defined as cumulative fracture length/fossae length per HiRISE image. The total number of pixels constituting the mapped fracture traces is a proxy for cumulative fracture length. The cumulative fossae length within each HiRISE image was calculated similarly. The results show that fracture intensity is highest in relays between fossae segments and sub-segments (Fig. 4). The highest fracture intensities along the fossae coincide with where Athabasca Valles appears to originate at the fossae. Further east, regions of mechanical interaction become fewer, and Fig. 4 shows a corresponding decrease in the fracture intensities, consistent with the results of [13] in terrestrial systems.

We note that lava, dust, and aeolian coverage likely obscure fractures. This is particularly problematic in this region because of the high dust abundance. Also, two HiRISE images in the dataset are at a lower map-projected resolution of 50 cm/px rather than 25 cm/px. Thus, fracture intensity calculations represent minimum values.

Conclusions: The depth profiles of the Cerberus Fossae are consistent with the displacement distribution of terrestrial normal faults with a surface expression consistent with fault propagation from depth and mechanical interaction among segments. Similarly, regions of interpreted mechanical interaction indicated by slip distribution and segment overlap correspond to increased fracture intensity. On Earth, such regions of mechanical interaction tend to have high fracture intensity [e.g. 13], are associated with hydrothermal fluid flow [9], and have evidence of extensive long-term fluid flow as evidenced by diagenetic alterations [8]. Higher fracture intensities near the head of Athabasca Valles as a proxy for increased permeability provide a potential mechanism and a necessary condition for the localized fluid flux necessary to supply the outflow channel.

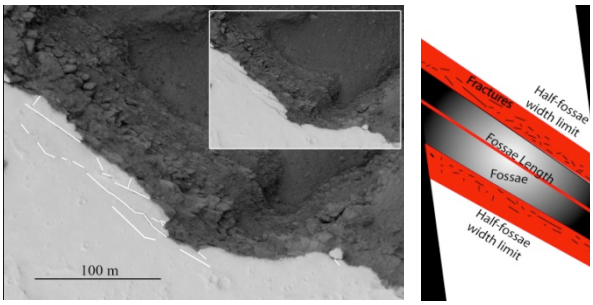

Fig. 3: *Left:* Example of fracture identification. Interpreted fractures from inset shown as white lines. Subimage of HiRISE PSP_004006_1900. Image credit: NASA/JPL/U of Arizona. *Right:* Cartoon of the sampling method.

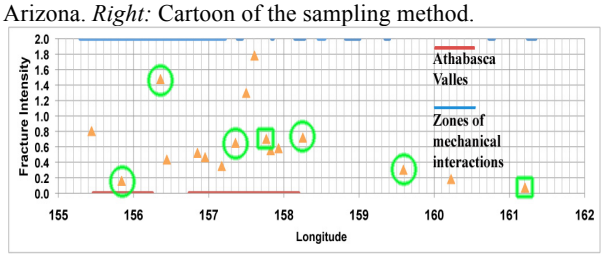

Fig. 4: Plot of fracture intensity versus longitude. The red and blue bars indicate Athabasca Valles and zones of mechanical interaction, respectively. Green ovals represent areas with higher aeolian dune coverage and therefore represent minimum intensities. Green squares represent HiRISE data collected from 50 cm/pixel rather than typical 25 cm/pixel images and so represent minimum intensities.

References: [1] Head J. W. et al. (2003) *Geophys. Res. Lett., 111,* **31**-1–**31**-4. [2] Burr D. et al. (2002) *Icarus, 159,* 53-73. [3] Carr, M. (2006) *The Surface of Mars*, Cambridge, 87-88. [4] Wyrick D. et al. (2004) *JGR, 109*. [5] Burr D. et al. (2002) *Geophys. Res. Lett., 29,* **13**-1–**13**-4. [6] Davatzes, A.K. and Gulick, V.C. (2007) *LPSC XXXVIII,* Abstract #1788. [7] Willemse and Pollard (1998) *JGR*, 103, 2427. [8] Eichhubl, P. et al. (2004) *GSA Bull., 116,* 1120-1136. [9] Curewitz, A., and Karson, J.A. (1997) *J. Volcan. & Geothermal Res., 79,* 149-168. [10] Peacock, D.C.P. et al. (1991) *J. Struct. Geo., 13,* 721-733. [11] Scholz, C. H (2002) *The Mechanics of Earthquakes and Faulting, 2nd ed.*, Cambridge, 126-127. [12] Contreras, J., et al. (2000) *J. Struct. Geo., 22,* 159-168. [13] Davatzes N. C. (2005) *GSA Bull., 117,* 135-148.